First European Conference on Earthquake Engineering and Seismology
(a joint event of the 13th ECEE & 30th General Assembly of the ESC)
Geneva, Switzerland, 3-8 September 2006
Paper Number: 275

A METHODOLOGY FOR DERIVATION OF SEISMIC FRAGILITY CURVES FOR BRIDGES WITH THE AID OF ADVANCED ANALYSIS TOOLS

Andreas KAPPOS[1], Ioannis MOSCHONAS[2], Themelina PARASKEVA[3] and Anastasios SEXTOS[4]

SUMMARY

Advanced inelastic analysis tools developed by the authors that include, among others, modal pushover analysis based on appropriately selected monitoring points for drawing the pushover curves and utilising the popular demand and capacity spectra approach, and time history analysis accounting for the influence of spatial variability of earthquake ground motion on both straight and curved bridges, are briefly presented. These tools are then used in the frame of a methodology for analytically deriving fragility curves for different types of bridges; two such case studies are presented herein, involving two different types of actual bridges.

1. INTRODUCTION

Within the framework of a major research programme in Greece ('ASProGe: Seismic Protection of Bridges') coordinated by the Laboratory of Concrete and Masonry Structures of the Aristotle University of Thessaloniki, the need arose for deriving seismic fragility curves for all types of bridges commonly found in the motorway system of Greece; these bridges can be considered as representative of current seismic design practice in Southern Europe. The ensuing fragility curves will be used, among other applications, as part of the seismic risk management system of the bridges along the 680km long Egnatia Motorway in Northern Greece (some of which are instrumented within the framework of the ASProGe project).

Several methods are currently being tested for producing fragility curves for a total of ten different types of concrete bridges, identified as the most common ones in Egnatia. The analysis of these bridges is carried out using advanced inelastic tools developed by the authors, which include, among others:

- Modal pushover analysis based on appropriately selected monitoring points for drawing the pushover curves, and the popular demand and capacity spectra approach.
- Time history analysis accounting for the influence of spatial variability of earthquake ground motion on both straight and curved bridges, as well as of soil-foundation-superstructure interaction.

The paper gives an overview of both the key features of the aforementioned advanced analysis tools and of the method used for deriving fragility curves; the latter are drawn assuming a lognormal distribution, and constructing the basic relationship between intensity of ground motion and bridge damage state using either pushover analysis or dynamic time history analysis. Damage state threshold values for the fragility curves are defined differently in bridges with yielding piers (of the column type), and bridges with elastomeric bearings and non-yielding piers of the wall type. Two examples of fragility curves will be presented, one for each of the aforementioned types (Krystallopigi Bridge and Lissos Bridge, respectively).

[1] Professor, Department of Civil Engineering, Aristotle University of Thessaloniki
Email : ajkap@civil.auth.gr
[2] Civil Engineer (MSc), PhD Candidate, Department of Civil Engineering, Aristotle University of Thessaloniki
Email : jfmoschon@kat.forthnet.gr
[3] Civil Engineer (MSc) , PhD Candidate, Department of Civil Engineering, Aristotle University of Thessaloniki
Email : thparask@civil.auth.gr
[4] Lecturer, Department of Civil Engineering, Aristotle University of Thessaloniki
Email : asextos@civil.auth.gr

2. APPLICATION OF ADVANCED ANALYSIS TOOLS TO SEISMIC ASSESSMENT OF BRIDGES

2.1 Advanced pushover procedures

Non-linear time-history analysis is the most rigorous method for estimating dynamic response of a bridge but it remains impractical because of the large workload and the complex procedure. On the other hand, the non-linear static procedure is used widely because of the conceptual simplicity and the computational attractiveness. A fundamental mode-based (Standard) pushover analysis cannot account for the contribution of higher modes to response which is an important limitation for the long-span bridges and bridges with high piers. Extension of the 'standard' pushover analysis (SPA) to consider higher modes effects has attracted attention, the effort being to match as closely as possible the results of nonlinear time history analysis. In order to consider the effects of the high modes, modal pushover method was developed. According to the Modal Pushover Analysis procedure [Chopra and Goel, 2002], standard pushover analysis is performed for each mode independently, wherein the elastic modal forces are applied as invariant seismic load patterns. Modal pushover curves are then plotted and can be converted to capacity diagrams. Response quantities are separately estimated for each individual mode, and then superimposed using an appropriate modal combination rule. The basic steps of the method have been presented by [Chopra and Goel, 2002], but a set of additional assumptions and decisions regarding alternative procedures that can be used are needed in order to apply the method in the case of bridges; a key issue is the selection of an appropriate point for monitoring the displacement demand (and also for drawing the pushover curve for each mode), other issues include the way a pushover curve is bilinearised before being transformed into a capacity curve, the use of the 'capacity spectrum' for defining the earthquake demand for each mode and then combining modal responses, and the number of modes that should be considered in the case of bridges. The basic steps of the Modal Pushover Analysis procedure for bridges, described in more detail in [Kappos et al., 2004b and Paraskeva et al., 2006] are summarised below.

At first pushover analysis is performed for *each* mode (n) independently, wherein the elastic modal forces are applied as invariant seismic load patterns. Modal pushover curves (V_{bn}-u_{rn}) are then plotted. Each one of the pushover curves has to be idealized as a bilinear curve (Fig.1-left), in order to define a yield point and ductility factor. The idealized V_{bn} - u_{rn} pushover curve of the Multi-Degree-Of-Freedom (MDOF) system is then converted to a spectral acceleration (S_a) vs. spectral displacement (S_d) plot ('spectrum'), of an equivalent Single-Degree-Of-Freedom (SDOF) system, using the relationships [Chopra and Goel, 2002]:

$$S_a = \frac{V_{bn}}{M_n^*} \;;\quad S_d = \frac{u_{rn}}{\Gamma_n \varphi_{rn}} \tag{1}$$

wherein φ_{rn} is the value of φ_n at the reference (or 'monitoring') point, $M_n^* = L_n \cdot \Gamma_n$ is the effective modal mass, $L_n = \varphi_n^T \cdot m \cdot 1$, $\Gamma_n = L_n / M_n$ and $M_n = \varphi_n^T \cdot m \cdot \varphi_n$ is the generalized mass, for the *n*th natural mode.

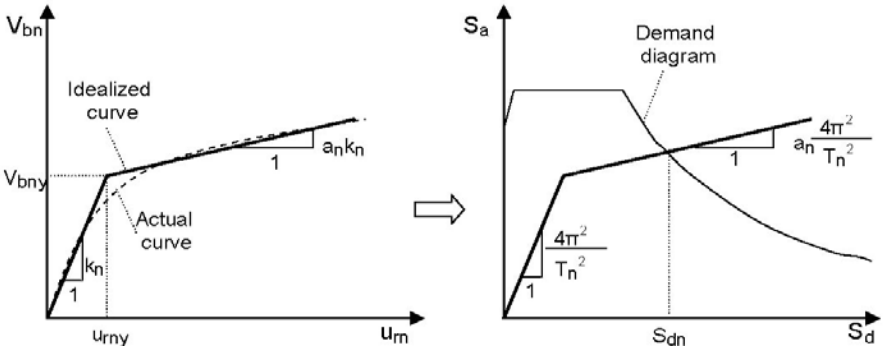

Figure 1: Idealized pushover curve of the *n*-th mode of the MDOF system and corresponding capacity curve for the *n*-th mode of the equivalent inelastic SDOF system.

Natural choices for the monitoring point in a bridge are the deck mass centre [Eurocode 8, EN 1998-2: 2004], or the top of the nearest to it pier, if the displacement of the two is practically the same, i.e. for monolithic or hinged pier-to-deck connections, but not for sliding or flexible connections. By analogy to building structures, it can also be selected as the point of the deck that corresponds to the location (x_n^*) of the equivalent SDOF system along the longitudinal axis of the bridge, defined by the location of the resultant of the modal load pattern $s_n^* = m \cdot \varphi_n$, which can be calculated from the properties of the MDOF system using the following relationship:

$$x_n^* = \frac{\sum_{j=1}^{N} x_j m_j \varphi_{jn}}{\sum_{j=1}^{N} m_j \varphi_{jn}} \tag{2}$$

in which, x_j is the distance of the j^{th} mass from a (selected) point of the MDOF system (in a bridge, the left abutment is a natural choice), and φ_{jn} is the value of φ_n at the jth mass; x_n^* is essentially independent of the way the mode is normalized.

Another proposal [Fischinger et al., 2004] for the monitoring point of the bridge is at the point of the deck where the (current) displacement is maximum, while in the present study the top of the pier that exhibits the most critical plastic rotation (again, for identical pier and deck displacements), which doesn't have to be the same for all individual analyses (i.e. for all modes) was also used. The selection of the monitoring point affects the shape of the pushover curve, as well as the second branch of the capacity curve; however it does not affect the initial branch of the capacity curve, whose slope is equal to ω_n^2 (i.e. the square of the circular frequency of the considered mode) if the initial slope of the corresponding pushover curve reflects the elastic (effective) stiffness properties of the bridge. Alternative pushover curves (referring to the transverse response of the bridge described in §4.1) are shown in Figures 2 and 3, with respect to the deck displacement at different locations; it is noted that the two procedures shown in Fig. 3 give similar results, which differ from those in Fig. 2 for some higher modes.

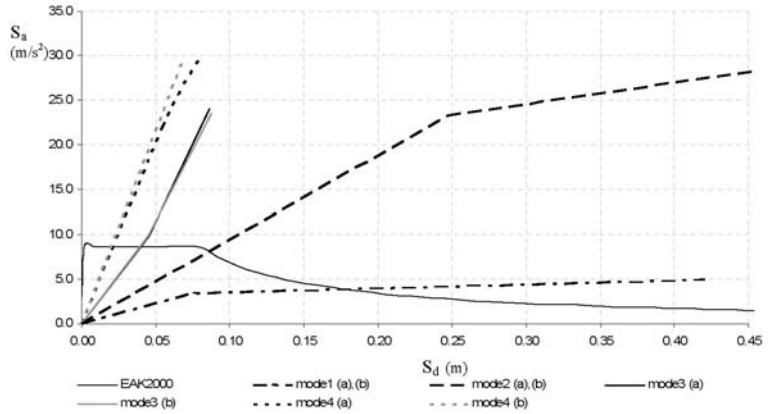

Figure 2: Capacity curves derived with respect to the deck displacement: (a) at the location of the deck mass centre; (b) at the location of the resultant of the modal forces for the four transverse modes (the elastic spectrum of the design earthquake is shown as 'EAK2000').

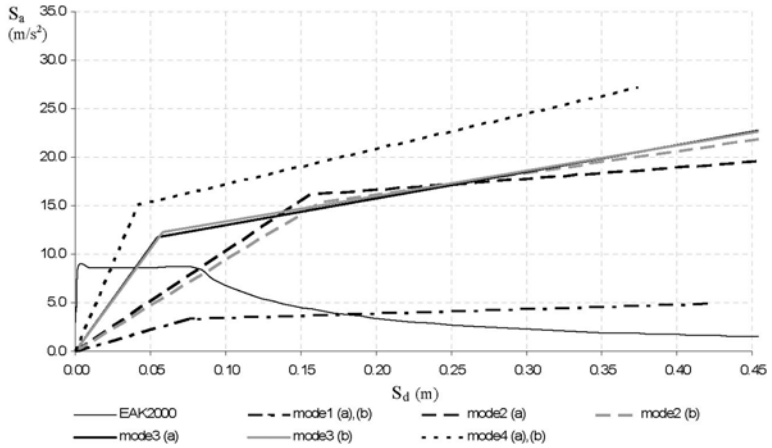

Figure 3: Capacity curves derived with respect to the deck displacement: (a) at the location of the most critical pier for each mode; (b) at the location of the current maximum displacement.

2.2 Non-linear time-history analysis accounting for spatial variability effects

The above advanced pushover procedures are often comparatively used with non-linear time history analyses. A computationally cost-effective, yet accurate, way to account for the potential lumped plastic behaviour at the base and the top of the piers in the time domain, is the use of non-linear rotational spring elements with a corresponding (bi-linear hardening) moment-rotation (M-θ) relationship which depends on the calculated ultimate moment and the input parameters defined from fibre analysis for each particular pier section. However, during strong ground motion, it is also expected that bridge structures are subjected to excitation that is non-uniform along their longitudinal axis in terms of amplitude, frequency content and arrival time, a fact primarily attributed to the wave arrival delay, their loss of coherency and the effect of local site conditions. Hence, advanced analytical solutions and enhanced know-how has to be utilized in order to identify the relative importance of the aforementioned phenomena and investigate potential implications in engineering design. Various analytical solutions for generating spatially variable seismic motions have been proposed, establishing the scientific background for analytically assessing long bridge structures. Particularly towards the inelastic dynamic behaviour of bridges, a set of parametrically modified realistic bridge structures [Nutti & Vanzi, 2005, Sextos et al., 2003] has also been studied, the latter study additionally accounting for the coupling effect of spatial variability, site effects and soil-structure interaction.

The comprehensive methodology developed by the authors has been utilised for the assessment of skewed bridges and the identification of the degree to which the bridge curvature affects the sensitivity of the structure to the assumptions of asynchronous motion. It was observed [Sextos et al., 2005] that both the elastic and inelastic dynamic response of multiply excited curved bridges is strongly dependent not only on the spatial variation of ground motion parameters but also on the frequency content of earthquake ground motion and the angle of incidence of the incoming wave field, as further elaborated in section 4.1. Such dynamic response discrepancy has been found that is in turn reflected to the inertial vibration of the foundation itself [Sextos et al., 2005] as well as on the resulting fragility curves, compared to those that would have been derived using the common assumption of synchronous excitation [Lupoi et al, 2005]. As a result, both earthquake input characteristics and the reinforced concrete (R/C) section non-linear parameters required for the analysis have to be carefully selected in order to enhance the reliability of the assessment procedure.

3. DERIVATION OF FRAGILITY CURVES

3.1 Overview of proposed procedure

In recent years several procedures have been proposed for the derivation of fragility curves either empirical [Basöz et al., 1999, Shinozuka et al., 2000b] or analytical [Hwang et al., 2000, Shinozuka et al., 2000a,b, Mander and Basöz, 1999, Gardoni et al., 2003]. The analytical procedures differ according to the method of analysis (nonlinear static or dynamic analysis), the earthquake parameter used for plotting fragility curves (peak ground acceleration-*PGA*, spectral displacement-S_d or spectral acceleration-S_a) and the choice of the probability density function (e.g. estimation of the variance). The procedure proposed here is based on *nonlinear static (pushover) analysis* in combination with the so-called *capacity spectrum method* and a definition of the damage states utilising the capacity curves of the bridge. A key aspect of the proposed procedure is the classification of bridges in two main categories: bridges with yielding piers (of the column type) and bridges with bearings (with or without seismic links) and non-yielding piers of the wall type. In the former type of bridges the inelastic behaviour is developed due to the formulation of plastic hinges at the base (and the top) of the piers while in the latter type inelastic behaviour develops due to the inelastic behaviour of bearings (and seismic links), because in most cases the deck is supported by wall-type piers which remain in the elastic range even for strong earthquake events. The successive steps of the proposed method are described in the following sections.

3.2 Derivation of pushover and capacity curves

In the case of bridges with inelastic piers the derivation of pushover curves takes place by performing either a standard pushover analysis or a modal pushover analysis for each mode independently, as described previously (§2.1). In case the suggested modal pushover method is used, a ‘multi-modal’ curve is constructed by SRSS combination of the values from individual curves. The pushover curve is then idealized as a bilinear one (Fig.1-left), to define a yield point and ensuing ductility factors, and be converted to a capacity curve (Fig. 1-right), so that it can be superimposed on appropriately scaled demand spectra, to establish the thresholds of damage states in terms of earthquake demand. Examples of such curves were already given in section 2.1 (Figures 2 and 3).

In the case of bridges with bearings (with or without seismic links) and non-yielding piers the procedure for deriving pushover and capacity curves is slightly different. At first, only the pushover curve of the first mode is derived for both directions since the fundamental mode of the bridge is similar to the corresponding fundamental mode of the deck because the wall-type piers are much stiffer than the bearings and as a consequence has a significant participating mass ratio. In the longitudinal direction the first mode of the deck is a rigid body displacement. In the transverse direction the first mode of the deck has a sinusoidal shape or is a rigid body displacement/rotation, depending on whether the deck transverse displacement at the abutments is blocked or not. Furthermore, there is no need for bilinear idealization of the capacity curve since the derived pushover and capacity curves have already a bilinear shape because of the corresponding bilinear behaviour of bearings (Fig. 4a, 4b-dashed line). In the presence of seismic links the pushover curve has a similar shape, but an apparent hardening/softening is noticed, due to successive activation and failure of the seismic links, respectively (Fig. 4b-continuous line). Finally, in the case of common elastomeric bearings the bilinear behaviour can be represented by a simple quasi-elastic behaviour given that the hysteresis loop of these bearings is very thin because of their low damping ratio (5%).

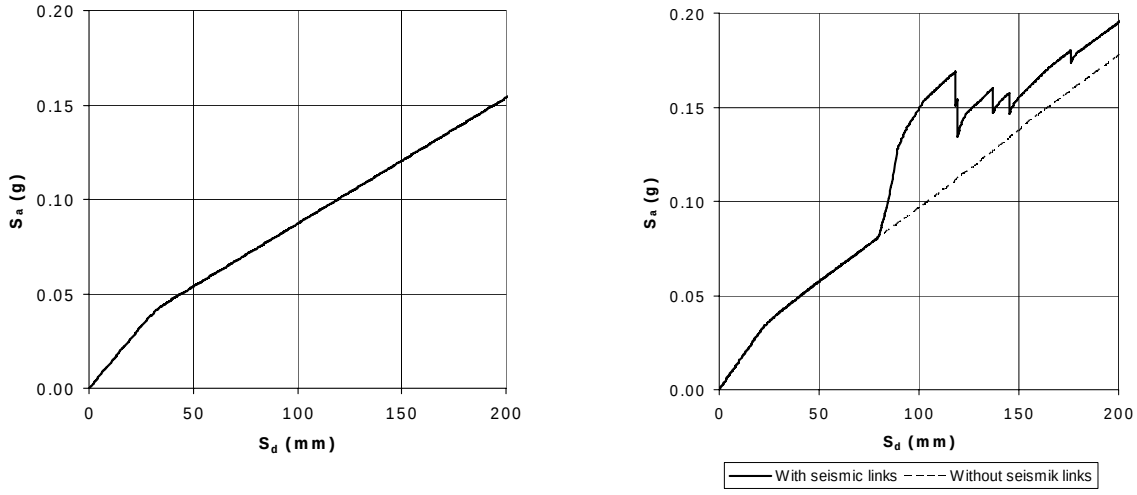

(a) Longitudinal direction (b) Transverse direction

Figure 4: Capacity curves of a bridge with bearings and non-yielding piers.

3.3 Definition of damage states

In the case of bridges with inelastic piers damage states can be defined on the basis of the idealized capacity curve of the bridge. In line with [Basöz et al., 1999], wherein analytical fragility curves were validated against empirical fragility curves obtained from actual bridge damage data, five damage states are considered: none, minor/slight, moderate, major/extensive damage and collapse. The description of these damage states and the corresponding values of the ratio δ/δ_y, are given in Table 1. For their definition, specific values of the bridge displacement were considered, such as the yield displacement δ_y and the ultimate displacement $\delta_u=\mu_u\cdot\delta_y$ (the former is critical for the lower damage states, while the latter is critical for the higher damage states). At this point it is worth mentioning that δ, δ_y and δ_u refer to the entire bridge, not to a single pier; obviously such a convenient description is more valid in the case of uniform distribution of damage along the bridge.

In the case of bridges with bearings (with or without seismic links) the definition of damage states starts from the shear deformation of bridge bearings, γ_{bi}. Five damage states are determined, as before (none, minor/slight, moderate, major/extensive damage and collapse). Then, the corresponding damage states of the single bearing i are defined in accordance with Table 2, based on a combination of (limited) test data from manufacturers, code values, and engineering judgement. Given the values for individual bearings at each damage state, a global shear deformation γ_g can be calculated as an average value for all bridge bearings, using the following relationship:

$$\gamma_g = \frac{\sum_{i=1}^{N} \gamma_{bi}}{N} \tag{3}$$

Table 1: Definition of damage states for bridges with inelastic piers

A/A	Damage state	Repairs Required	Outage Expected	Threshold Values [δ/δ_y]
DS0	None	None	---	<0.7
DS1	Minor/Slight	Inspect, adjust, patch	<3 days	>0.7
DS2	Moderate	Repair components	<3 weeks	>1.5
DS3	Major/Extensive	Rebuild components	<3 months	>3
DS4	Collapse	Rebuild structure	>3 months	>μ_u

Table 2: Definition of damage states for the single bearing

A/A	Damage state	Threshold Values [γ_{bi}]	Damage State Limits [γ_{bi}]
DS0	None	$\gamma<\gamma_y$=0.2	$0\leq\gamma<\gamma_y$=0.2
DS1	Minor/Slight	$\gamma>\gamma_y$=0.2	γ_y=0.2$\leq\gamma$<1.5
DS2	Moderate	γ>1.5	1.5$\leq\gamma$<2.0
DS3	Major/Extensive	γ>2.0	2.0$\leq\gamma$<5.0
DS4	Collapse	γ>5.0	$\gamma\geq$5.0

where N is the total number of bridge bearings and γ_{bi} is the shear deformation of the single bearing i. The definition of damage states for the whole bridge according to the total shear deformation γ_{tot}, is similar to the definition of damage states of the single bearing (Table 2).

It is seen from Tables 1 and 2 that the definition of damage states in the proposed procedure is made in terms of damage parameters (which in the case of bridges with inelastic piers is the ratio δ/δ_y whereas in the case of bridges with bearings the global shear deformation γ_g), rather than in terms of damage indices (e.g. percent of loss in capacity or of residual capacity), an option that enables a convenient definition of the Minor/Slight damage state (in terms of damage index, any non-zero value would imply entering this damage state).

3.4 Estimation of fragility curve parameters

In line with other similar proposals [FEMA-NIBS, 2003], fragility curves in the proposed procedure are expressed by the lognormal cumulative probability function:

$$F\left(DP \geq DP_i \mid S\right) = \Phi\left[\frac{1}{\beta_{tot}} \cdot \ln\left(\frac{S}{S_{mi}}\right)\right] \tag{4}$$

wherein $F(\cdot)$ the probability of the damage parameter (DP) being or exceeding the value DP_i for the i-th damage state (Tables 1 and 2) for a given ground shaking level defined by the earthquake parameter S (Peak Ground Acceleration-PGA or Spectral Displacement S_d), Φ is the standard normal cumulative probability function, S_{mi} the median threshold value of the earthquake parameter S so as to cause the i-th damage state and β_{tot} the total lognormal standard deviation.

Only two parameters are needed to describe the fragility curve expressed by (5), S_{mi} and β_{tot}. The estimation of S_{mi} is based on the capacity spectrum method, wherein the demand spectrum (in spectral acceleration vs. spectral displacement format) is superimposed on the same plot with the capacity curve of the bridge. It is noted that the demand spectrum is plotted for a range of values of the earthquake parameter S (Fig. 5). Peak ground acceleration (PGA) is used as earthquake parameter in this study, but spectral quantities can also be used. Fig. 5a shows the general case of the capacity spectrum method, while Fig. 5b shows the case in which the fundamental period of the bridge T is longer than about 0.5 to 0.6 sec (the range of periods wherein the equal displacement rule is a reasonable assumption). Using the intersection points of the capacity and demand curves, the diagram of

Fig. 6 can be plotted (evolution of damage with earthquake intensity), in which the horizontal axis is the earthquake parameter S (taken here as the PGA) and the vertical axis is the damage parameter DP (δ/δ_y or γ_g). Then, using the evolution of damage diagram and the definitions of Tables 1 and 2, the median threshold value of the earthquake parameter S_{mi} (here PGA_{mi}) for each damage state can be obtained. For example the threshold value of PGA for the damage state DS2 (moderate damage) for bridges with inelastic piers is that corresponding to δ/δ_y=1.5 (see Table 1), whereas for bridges with bearings (with or without seismic links) the value of PGA corresponding to γ_{tot}=1.5 (Table 2).

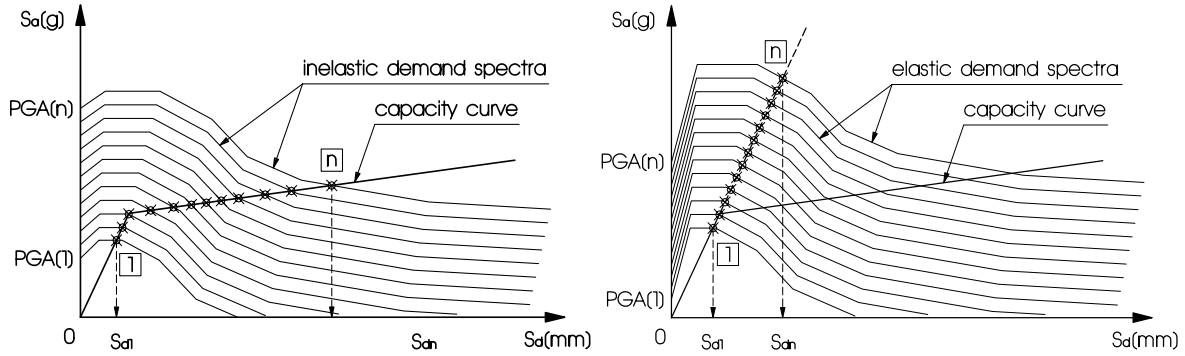

Figure 5: Capacity spectrum method

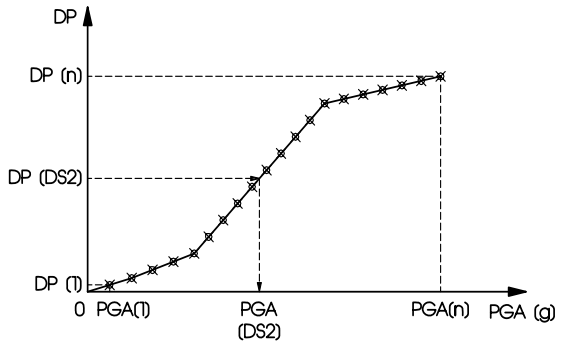

Figure 6: Damage-earthquake parameter diagram

The second parameter of Eq. (5) is the total lognormal standard deviation β_{tot}, which takes into account the uncertainties in seismic input motion (demand), the uncertainties in response and resistance of the bridge (capacity) and the uncertainties in the definition of damage states. This parameter (β_{tot}) can be estimated by SRSS combination of the individual uncertainties (in demand, capacity, and damage state definition) assuming these are statistically independent. The value of β_{tot} was calibrated by [Dutta and Mander, 1998] using a theoretical approach and validated by [Basöz and Mander, 1999] on the basis of empirical fragility curves obtained from actual bridge damage data gathered from Loma Prieta (1989) and Northridge (1994) earthquakes. According to these studies the value of β_{tot} was set to 0.6; in the absence of a more accurate estimation of uncertainties in capacity, demand and damage states, β_{tot}=0.6 is used at this stage of development. Further work in this direction is planned in the framework of the previously mentioned research project (ASProGe).

4. APPLICATION TO ACTUAL BRIDGES

4.1 Krystallopigi Bridge

The selected Krystallopigi Bridge is a twelve span structure of 638m total length that crosses a valley in west-northern Greece, and is characterised by a large curvature in plan (radius equal to 488m). The deck consists of a 13m wide prestressed concrete box girder section. Piers are rectangular hollow reinforced concrete members. The structure is supported on 11 piers of heights between 11 and 27m. The support of the deck on the piers follows a rather complex, albeit not uncommon in modern bridges in seismic areas like Greece, pattern wherein for the outer piers 1, 2, 3, 9, 10, and 11 a bearing-type pier-to-deck connection is adopted, allowing movement in

the longitudinal (tangential, due to the curved configuration) direction, but restricting movement in the transverse (radial) direction, while the inner (taller) piers 4 to 8 are monolithically connected to the deck. The piers are supported on pile groups of length and configuration that differ between supports due to the change of the soil profile along the bridge axis. More construction details of the Krystallopigi Bridge can be found in previous studies [Kappos et al., 2004b, Paraskeva et al., 2006].

After carrying out analyses using the Modal Pushover Procedure (see §2.1, Fig.2 and 3), it was decided to draw the capacity curve of the first mode in both directions in terms of the deck displacement at the central pier location (Fig. 7) to derive fragility curves comparable with those derived for bridges with bearings (with or without seismic links) and non-yielding piers (Lissos Bridge, see §4.2). As demand spectrum the elastic spectrum of the 2003 Greek Seismic Code for soil class B was used. The value for β_{tot} was 0.6 (see section 3.4). Fig. 8 shows the derived fragility curves for Krystallopigi Bridge.

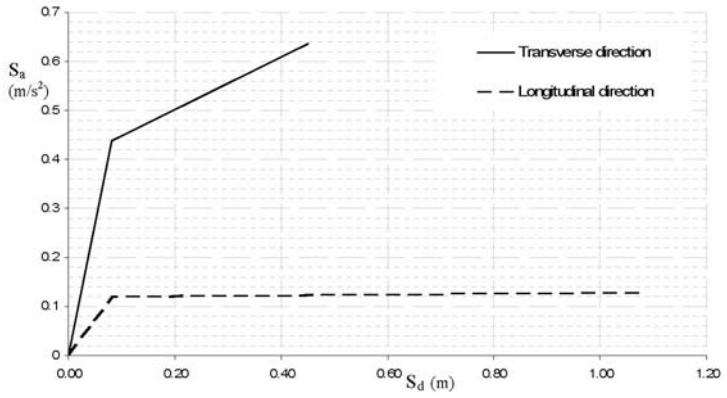

Figure 7: Capacity curves derived with respect to the deck displacement at the location of the central pier in both directions of the bridge.

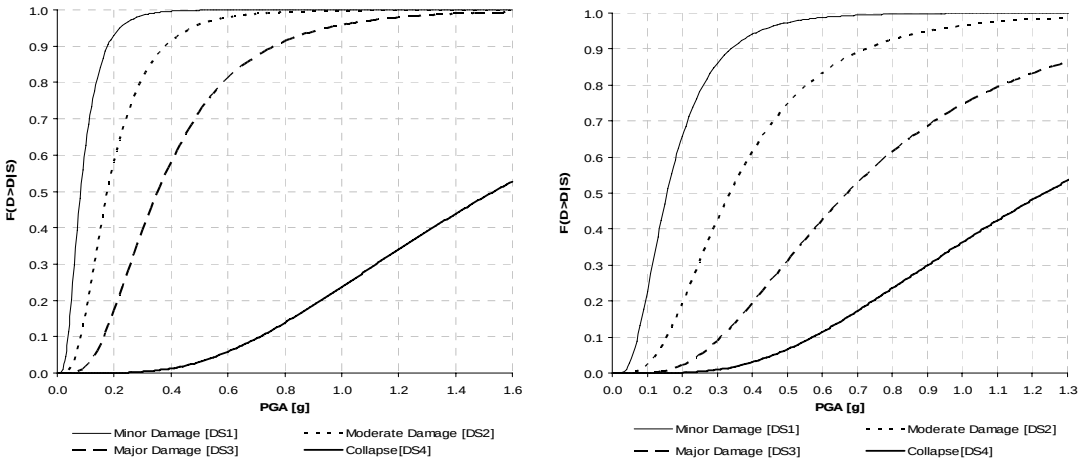

(a) Longitudinal direction (b) Transverse direction

Figure 8: Fragility curves for Krystallopigi Bridge.

It is seen in Fig. 8 that the distance between fragility curves of the last damage state (DS4) and the other three damage states (DS1, DS2 and DS3) is much greater in the longitudinal direction than in the transverse one, reflecting the significant difference in the available ductility μ_u in the two directions (see Fig. 7). Furthermore, in both directions the median threshold value PGA_{mi} for the collapse damage state (DS4) is approximately the same. This means that the possibility of the bridge to collapse is also approximately the same in both directions (since β_{tot} was taken equal to 0.6 for either the transverse or the longitudinal direction). This can be explained referring to the capacity curves of the two directions; as Fig. 4 shows, the bridge in the longitudinal direction has higher ultimate ductility than in the transverse, with approximately the same ratio that in the transverse direction ultimate strength is larger than in the longitudinal. Finally, the ratio of the ultimate strength between the two directions affects the corresponding median threshold values and fragility curves of DS1, DS2 and DS3 damage states. Consequently, in the longitudinal direction there is a higher probability to develop minor/slight, moderate

and major/extensive damage than in the transverse direction, for a given level of *PGA*. Finally, it is noted that the dynamic response of the Krystallopigi bridge, has been found to be sensitive to the application of spatially variable earthquake input and (to a lesser extent) to the angle of incidence of the incoming seismic waves [Sextos et al., 2004]. In view of this, the sensitivity of the derived fragility curves to the selection of the (asynchronous) loading pattern is currently being investigated.

4.2 Lissos Bridge

The bridge, crossing the river Lissos (in N-E Greece), is an 11-span structure of 430m total length. The deck consists of a 13m wide prestressed concrete box girder section and is supported on ten wall-type piers of heights between 4.5 and 10.6m through elastomeric bearings. Deck movement at the abutments is free in the longitudinal direction and blocked in the transverse. The pier section is solid rectangular 2.5×6.5m with rounded edges. At the top of the piers there are seismic links 1.2m high, to limit the deck transverse displacement in the case of a strong earthquake by developing plastic hinges at the link. The link section is a cyclic sector with a depth varying from 0.50m at the base to 0.30m at the top. The piers are supported on pile groups of length and configuration that differ between supports due to the change of the soil profile along the bridge axis. It is worth mentioning that Lissos' is the first bridge in Greece constructed using the incremental launching method.

According to the proposed procedure, the capacity curves (S_a-S_d) of the 1st mode in the longitudinal and transverse direction were derived (Fig.4). As demand spectrum the elastic spectrum of the Greek Seismic Code Version 2000 for soil class C was used. Threshold values of PGA_{mi} are 0.04g, 0.28g, 0.37g and 0.93g for damage states DS1, DS2, DS3 and DS4, respectively for the longitudinal direction while for the transverse direction the corresponding values are 0.06g, 0.44g, 0.58g and 1.45g. Fig. 9 shows the derived fragility curves, and it is noted that fragility curves of moderate and major/extensive damage states are closely spaced, which reflects the corresponding small distance between the median threshold values of the damage parameter γ_{tot} (Table 2). It is also seen that the probability of the bridge exceeding a damage state for a given seismic level is greater in the longitudinal direction than in the transverse one. This is anticipated on the basis of the median threshold values of PGA_{mi} in the two directions, and can be explained by taking into account the definition of the total shear deformation γ_{tot}, i.e. it is the average value among all bridge bearings and is influenced by the type of deck movement in each direction. In the longitudinal direction the deck moves as a rigid body, hence all bearings have the same displacement, and the total shear deformation γ_{tot} is nearly equal to the deformation of the single bearing γ_{bi}. In contrast, in the transverse direction the deck deformation follows the sinusoidal shape of the transverse fundamental mode, hence the deformation of the bearings varies significantly from the middle of the bridge to the abutments, and consequently γ_{tot} is smaller than the max deformation of single bearings.

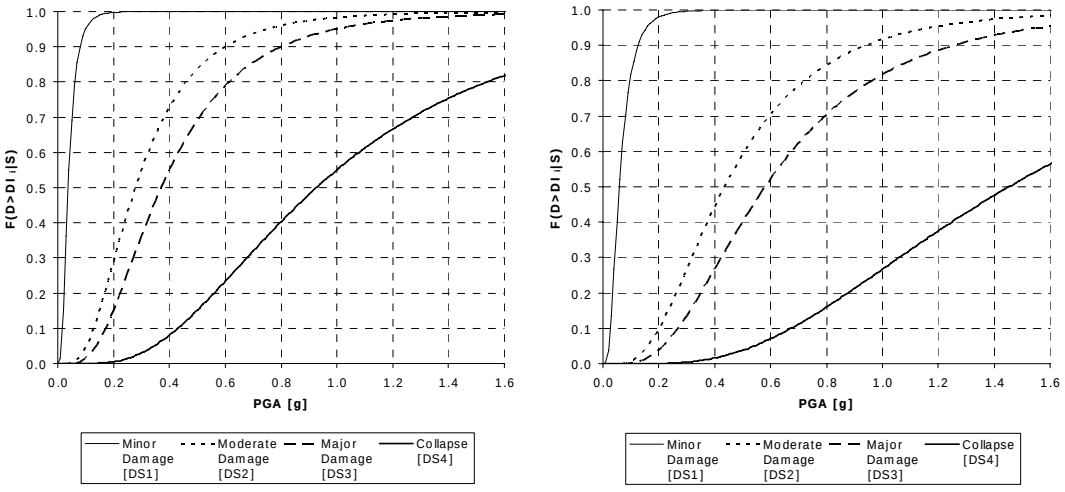

(a) Longitudinal direction (b) Transverse direction

Figure 9: Fragility curves for Lissos Bridge.

5. CONCLUSIONS

The present stage of development of advanced inelastic analysis tools by the authors, which include, among others, modal pushover analysis based on appropriately selected monitoring points for drawing the pushover

curves and the popular demand and capacity spectra approach, and time history analysis accounting for the influence of spatial variability of earthquake ground motion on both straight and curved bridges, were briefly presented. Inelastic analysis tools were then used in the frame of a methodology for analytically deriving fragility curves for different types of bridges. The different procedure for the definition of damage states in the case of bridges with yielding piers, as opposed to those with yielding bearings, was one of the key proposals of the present study. Application of the proposed procedure to the derivation of fragility curves for two actual bridges (on the Egnatia Motorway) with different seismic energy dissipation systems, has illustrated the applicability of the method in both types of bridges.

6. REFERENCES

Basöz, N.I., Kiremidjian, A.S., King, S.A., and Law, K.H. (1999), Statistical Analysis of Bridge Damage Data from the 1994 Northridge, CA, Earthquake, *Earthquake Spectra*, 15, n° 1.

CEN (Comité Européen de Normalisation) (2004), Eurocode 8: Design of structures for earthquake resistance – Part 2: Bridges (EN 1998-2: 2004), *CEN (Comité Européen de Normalisation)*, Brussels.

Chopra, A.K. and Goel, R.K. (2002), A modal pushover analysis procedure for estimating seismic demands for buildings, *Earthquake Engineering & Structural Dynamics*, 31, n° 3, 561-582.

Dutta, A., and Mander, J.B., (1998), Seismic Fragility Analysis of Highway Bridges, INCEDE-MCEER Center-toCenter, *Proceedings of the Center-to-Center Workshop on Earthquake Engineering Frontiers in Transport Systems*, Tokyo, Japan, 311-325.

FEMA-NIBS (2003), Multi-hazard Loss Estimation Methodology - Earthquake Model: HAZUS®MH Technical Manual, Washington DC.

Fischinger, M., Beg, D., Isakovic, T., Tomazevic, M. and Zarnic, R. (2004), Performance based assessment – from general methodologies to specific implementations. *Inernational Workshop on PBSD, Bled, Slovenia*, published in PEER Rep. 2004-05 (UC Berkeley), 293-308

Gardoni, P., Khalid, M.M., and Kiureghian, A.D. (2003), Probabilistic Seismic Demand Models and Fragility Estimates for RC Bridges, *Journal of Earthquake Engineering*, 7, n° 1, 79-106.

Hwang, H., Jernigan, J.B., and Lin, Y.W. (2000), Evaluation of Seismic Damage to Memphis Bridges and Highway Systems, *Journal of Bridge Engineering*, *ASCE*, 5, n° 4, 322-330.

Kappos, A.J., Panagiotopoulos, C., and Panagopoulos, G. (2004a), Derivation of fragility curves using inelastic time-history analysis and damage statistics, *ICCES'04 (Madeira, Portugal, July 2004)*, *CD ROM Proceedings, 665-672*.

Kappos, A., Paraskeva, T., Sextos, A. (2004b), Seismic assessment of a major bridge using modal pushover analysis and dynamic time-history analysis, *Advances in Computational & Experimental Engineering and Sciences*, Tech Science Press, 673-680.

Lupoi, A., Franchin, P., Pinto, P. E., and Monti, G. (2005) 'Seismic design of bridges accounting for spatial variability of ground motion', Earthq. Eng. Struct. Dyn, Vol. 34(4-5), 327-348.

Mander, J.B., and Basöz, N. (1999), Seismic Fragility Curve Theory for Highway Bridges, *Proceedings of the 5th U.S. Conference on Lifeline Earthquake Engineering*, *Paper 16*.

Nutti, C. and Vanzi, I. (2005), Influence of earthquake spatial variability on differential soil displacements and SDF system response, *Earthquake Engineering and Structural Dynamics*, 34 n° 11, 1353-1374.

Paraskeva, T., Kappos, A., Sextos, A. (2006), Extension of modal pushover analysis to seismic assessment of bridges, *Earthquake Engineering & Structural Dynamics*, 35, n° 11, 000-000.

Sextos A., Kappos A.. & Pitilakis K. (2003) 'Inelastic dynamic analysis of RC bridges accounting for spatial variability of ground motion, site effects and soil-structure interaction phenomena. Part 2: Parametric study', *Engineering and Structural Dynamics*, 32, 629-652.

Sextos, A., Kappos, A. and Mergos P. (2004) 'Effect of Soil-Structure Interaction and Spatial Variability of Ground Motion on Irregular Bridges: The Case of the Krystallopigi Bridge', *13th World Conference on Earthquake Engineering*, Vancouver, CD-ROM Volume, Paper No. 2298.

Sextos, A., Kappos, A. and Pitilakis, K. (2005) 'Recent developments on the effect of asynchronous earthquake excitation on the dynamic response of soil-foundation-superstructure bridge systems', *1st Greece – Japan Workshop: Seismic Design, Observation and Retrofit of Foundations*, 211-228.

Shinozuka, M., Feng, M.Q., Kim, H.K., and Kim, S.H. (2000a), Nonlinear Static Procedure for Fragility Curve Development, *Journal of Engineering Mechanics*, 126, n° 12, 1287-1295.

Shinozuka, M., Feng, M.Q., Lee, J., and Naganuma, T. (2000b), Statistical Analysis of Fragility Curves, *Journal of Engineering Mechanics*, 126, n° 12, 1224-1231.